polymers

MDPI

Article

A Quarterthiophene-Based Dye as an Efficient Interface Modifier for Hybrid Titanium Dioxide/Poly(3-hexylthiophene)(P3HT) Solar Cells

Arumugam Pirashanthan [1,2], Thanihaichelvan Murugathas [2], Neil Robertson [3], Punniamoorthy Ravirajan [2,*] and Dhayalan Velauthapillai [1,*]

1 Faculty of Engineering, Western Norway University of Applied Sciences, 5020 Bergen, Norway; pirashanthan.arumugam@gmail.com
2 Department of Physics, University of Jaffna, Jaffna 40000, Sri Lanka; thanihai@gmail.com
3 EaStCHEM School of Chemistry, University of Edinburgh, Edinburgh EH93FJ, UK; neil.robertson@ed.ac.uk
* Correspondence: pravirajan@gmail.com (P.R.); Dhayalan.Velauthapillai@hvl.no (D.V.); Tel.: +94-(0)-71-856-1715 (P.R.); +47-(0)-92-819-641 (D.V.)

Received: 1 October 2019; Accepted: 22 October 2019; Published: 25 October 2019

Abstract: This work focused on studying the influence of dyes, including a thiophene derivative dye with a cyanoacrylic acid group ((E)-2-cyano-3-(3′,3′′,3′′′-trihexyl-[2,2′:5′,2′′:5′′,2′′′- quaterthiophene]-5-yl) acrylicacid)(4T), on the photovoltaic performance of titanium dioxide (TiO_2)/poly(3-hexyl thiophene)(P3HT) solar cells. The insertion of dye at the interface improved the efficiency regardless of the dye used. However, 4T dye significantly improved the efficiency by a factor of three when compared to the corresponding control. This improvement is mainly due to an increase in short circuit current density (J_{SC}), which is consistent with higher hole-mobility reported in TiO_2/P3HT nanocomposite with 4T dye. Optical absorption data further revealed that 4T extended the spectral response of the TiO_2/P3HT nanocomposite, which could also enhance the J_{SC}. The reduced dark current upon dye insertion ensured the carrier recombination was controlled at the interface. This, in turn, increased the open circuit voltage. An optimized hybrid TiO_2/P3HT device with 4T dye as an interface modifier showed an average efficiency of over 2% under-simulated irradiation of 100 $mWcm^{-2}$ (1 sun) with an Air Mass 1.5 filter.

Keywords: hybrid solar cells; titanium dioxide; poly(3-hexylthiophene); oligothiophene dye; interface modifier; photovoltaic; absorption; quantum efficiency; polymers; efficiency

1. Introduction

Hybrid nanoporous metal-oxide polymer photovoltaic devices have been intensively studied for more than two decades, as these devices offer potential advantages relative to organic acceptors, such as low cost, facile synthesis via wet chemical processing, control of heterojunction morphology, and the potential for higher physical and chemical stabilities [1]. A metal-oxide nanoparticle (TiO_2, ZnO) percolation network with thickness in the submicron scale provides a stable and transparent backbone network for free carrier transport in this type of solar cells [2]. However, the power conversion efficiency (PCE) of these hybrid devices is limited due to several reasons, including interfacial carrier recombination [3,4] at the interface, poor mobilities in the metal-oxide polymer nanocomposite, and poor spectral response of the polymer [5–8]. Typically, the nanoporous metal oxides are the electron acceptors and the π-conjugated polymers are the donors [9–11] in hybrid metal-oxide polymer solar cells. The electron transfer from a donor into an acceptor produces a large proportion of charge carrier pairs across the donor/acceptor interface. In that situation, the Coulombic attraction of these bound charge carrier pairs limit the device performance by feeding the recombination effects at the

interface [8,12–14]. It has been shown that engineering the metal-oxide polymer interface can improve the PCE of hybrid solar cells [12,15–17]. Using nanolayers of absorber materials could improve the spectral response and reduce the interfacial recombination [18,19]. Organic dye molecules were also widely investigated as the interface modifier for metal-oxide polymer solar cells. In addition to a number of natural dyes [20–24], N719 and Z907 are two of the most common Ruthenium-based dyes successfully used as an absorber material in highly efficient dye-sensitized solar cells [25,26]. These dyes were also efficiently used as an interface modifier in solid-state hybrid solar cells and were found to improve the spectral response by participating in carrier generation, limiting the recombination [27] at the interface and hence improving both short circuit current density (J_{SC}) and the open circuit voltage (V_{OC}).

Planells M. et al. reported a series of thiophene derivative dyes with a cyanoacrylic acid group with conjugation length from one to five thiophene units (1T to 5T) as interface modifiers at TiO_2/P3HT solar cells [16]. These dyes are metal ion-free dyes and have an electron-rich thiophene group. It was found that the dyes improve the V_{OC} due to a dipole moment at the interface [16,28]. Oligothiophenes are discrete, monodisperse molecules, and are distinct from polythiophene, which inherently exists as a distribution of molecular weights. A pure carboxylated oligothiophene can be isolated from any unfunctionalized oligomers via column chromatography and recrystallization [28]. Such organic semiconducting oligothiophenes have been intensively investigated and widely used in organic photovoltaic (OPVs) due to the presence of excellent charge transport properties and tunable optical/electrochemical properties [29]. These tunable electrochemical properties were successfully investigated with variation of thiophene unit and show energy gap reduction when increasing the number of thiophene units from 1T to 5T [16,30].

The 4T dye at the interface was found to increase the hole-mobility in TiO_2/P3HT polymer nanocomposite by a magnitude of 10 times compared to the corresponding untreated nanocomposite. This is due to passivation of surface traps by the dye, as well as improved packing of the polymer with the nanocrystals through effective inter-chain interactions of 4T with P3HT [8]. The molar extinction coefficient (MEC) is an important parameter in defining the amount of material to be loaded on an electrode for maximum energy conversion, particularly at thin layers of the acceptors. It was also reported that the dyes with higher MEC can improve the stability of dye-based solar cells [31]. Given that the 4T dye can improve the performance of TiO_2-P3HT solar cells by involvement in photocurrent generation, the amount of dye molecules at the interface needs to be optimized. It was found that the MEC of 4T dye is higher than that of N719 and Z907 dyes. This work enhanced the performance of hybrid TiO_2/P3HT polymer solar cells by optimizing the device fabrication conditions with dyes and investigates the role of 4T dye at the metal-oxide polymer interface in enhancing the performance of hybrid TiO_2/P3HT polymer solar cells.

2. Materials and Methods

Solar Cell Fabrication: The solar cells were made using indium tin oxide (ITO) coated glass substrates (12 mm × 12 mm, 10 Ω/square). All the chemicals and solvents used in this work were purchased from Sigma Aldrich. The cleaned ITO substrates were first spray-coated with a diluted solution of titanium (iv) isopropoxide and acetylacetone mixture [8] in ethanol at a substrate temperature of 500 °C and baked at the same temperature for 30 min in order to form a ~50 nm-thick dense/blocking TiO_2 layer. Thereafter, a mesoporous TiO_2 layer was spin-coated on top of the dense TiO_2 with the solution (240 mg ml^{-1}) of TiO_2 paste (18NRT) (Dyesol, Queanbeyan, Australia) [30,32,33] dissolved in tetrahydrofuran [8] and allowed to sinter at 450 °C for 30 min [34]. As in previous studies [8,11,35], we used 0.3 mM concentrated dyes Z907 (Mw = 870.10), N719 (Mw = 1188.55), and 4T (Mw = 678.05) by dip-coating for 16 h at 90 °C in order to modify the mesoporous TiO_2 films. The chemical structures of the dyes and polymer used in this work are shown in Figure 1.

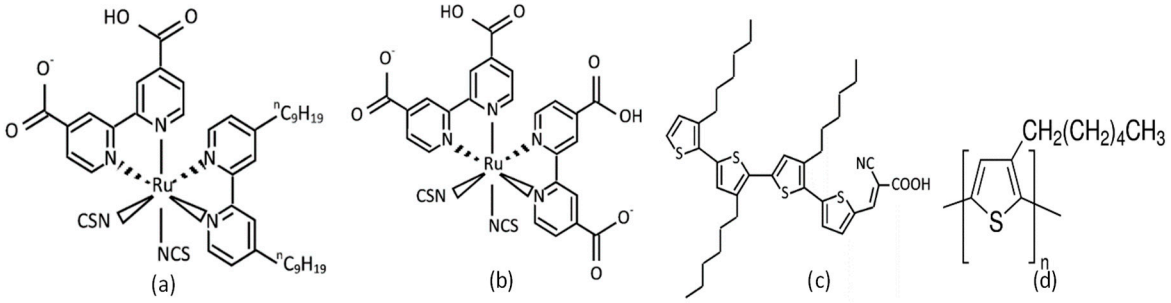

Figure 1. Chemical structure of dyes and polymer used: (**a**). Z907 [8], (**b**). N719 [8], (**c**). 4T [8,16], and (**d**) P3HT.

The influence of the concentration of the interface modifier on the device performance was examined with various concentrations of 4T dye. In each situation, the dye solutions were prepared using a 1:1 volume ratio solvent mixture of acetonitrile with tert-butanol [8,30,32]. After dye dipping, the electrodes were washed in 1:1 volume ratio mixture of acetonitrile with tert-butanol to remove excess dye in the nanoporous layer [8]. The dye-modified electrodes were first dip-coated with 2.5 mg ml^{-1} P3HT (Merck KGaA, Germany) and then spin-coated with (25 mg ml^{-1}) P3HT solution dissolved in chlorobenzene. Next, 100 nm of Gold top contact was deposited as described in [3,18,19] by thermal evaporation under high vacuum through an Edwards E306 thermal evaporator (Moorfield, Cheshire, UK). Finally, the fabricated solar cell devices were allowed to anneal process with nitrogen medium at 120 °C for 10 min in order to improve the interfacial characteristics [36].

Optical Characterization: Absorbance spectra of the dye-coated TiO_2 films were recorded using a JENWAY 6800 UV/Vis. Spectrophotometer (OSA, UK), which was controlled using Flight Deck software. The thickness of TiO_2 and P3HT layers were recorded by field emission scanning electron microscopy (FESEM, ZEIS Sigma, UK)

Electrical Characterization: The electrical characterization of both polymer and solid-state solar cells were tested, and the current-voltage curves were recorded with a computer-controlled Keithley 2400 source meter unit under the conditions of dark and 100 mW/cm^2 illuminations of the solar simulator (SCIENCE TECH, Ontario, Canada) with an Air Mass (AM) 1.5 spectral filter. The external quantum efficiency (EQE) measurements were carried out with a Monochromator (Newport, CA, USA) and a calibrated silicon photodiode (Newport, CA, USA).

3. Results

Figure 2a–c compares optical absorption spectra of dyes (4T, N719, and Z907) dissolved in tert-butanol and acetonitrile solution with 0.3 mM concentration, dye dip-coated nanoporous TiO_2 electrodes, and dye polymer dip-coated nanoporous TiO_2 electrodes. It is clear that the peak MEC of 4T dye is a factor of two higher than the other two standard dyes. P3HT has broader absorption spectrum in the visible region when compared to the metal-complex dyes, and the absorption spectrum of the 4T dye compliments the polymer absorption in the visible region. Figure 2 further shows that the polymer uptake and visible light absorption of the electrode treated with 4T dye was much higher than the electrodes treated with N719 and Z907 dyes. This is probably due to higher MEC of 4T and better compatibility between thiophene based dye and poly(3-hexyl thiophene). The combination of thiophene units of 4T with poly(3-hexyl thiophene) increased the overall thiophene units in the π-conjugated system, which led to the red-shifted and broadened absorbance spectrum under the UV/visible region [37].

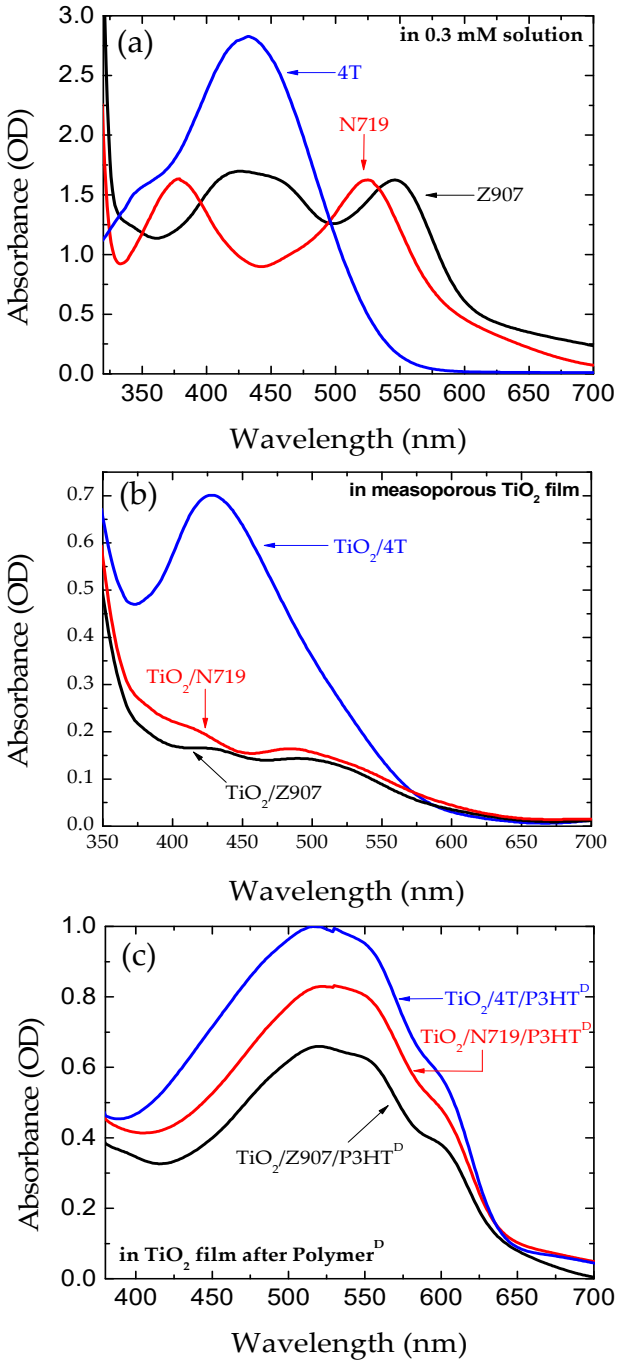

Figure 2. Optical absorption spectra of (**a**) 0.3 mM concentration of dyes dissolved in tert-butanol and acetonitrile solution, (**b**) dye dip-coated nanoporous TiO_2 electrodes, and (**c**) dye polymer dip-coated nanoporous TiO_2 electrodes.

To confirm the dimensions of the layer, we performed FESEM on the samples. A completed device was cut into two and the cross-section of the device was examined. The cross-sectional FESEM image of the completed device is shown in Figure 3. It clearly shows that thickness of the TiO_2/4T/P3HT nanocomposite was about 780 nm, in which about 150 nm excess polymer layer could serve as an electron blocking layer (to block direct contact between TiO_2 nanoparticles and top contact). For FESEM images of each layer, please refer to the Figures SM1–SM4 in the Supplementary Materials.

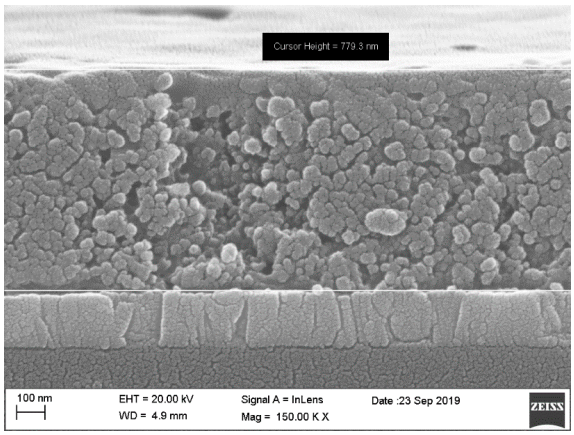

Figure 3. Cross-sectional field emission scanning electron microscopy (FESEM) image for the fabricated TiO_2/4T/P3HT solar cell.

Figure 4a and Table 1 clearly show that the insertion of dye molecules at the TiO_2/P3HT interface increased the short circuit current density (J_{SC}), open circuit voltage (V_{OC}), and subsequently the PCE. However, the devices with 4T dye-treated electrodes showed a maximum efficiency of about 2%, which was five-fold higher than that of the corresponding control TiO_2/P3HT devices without any dye treatment. This is mainly due to a four-fold increment in the J_{SC}. This can be attributed to increased hole-mobility of P3HT due to the insertion of 4T dye [8] at the interface between the TiO_2/polymer interface. Figure 4b shows that the dark current was significantly suppressed in dye-treated devices when compared with the corresponding control. This is an indication of reduced back electron transfer [38]. The lowest dark current was observed in 4T dye-treated devices, and was three orders of magnitude lower than that of the corresponding control device. This may suggest that the metal complex dyes have a more beneficial effect in shifting up the TiO_2 conduction band energy. Then, the external quantum efficiency (EQE) spectra of the dye-treated and untreated TiO_2/P3HT devices were measured. Figure 5 illustrates the EQE spectra of all devices tested. The conversion efficiency in polymer increased regardless of the dyes used. Figure 5 clearly shows that the influence of dyes N719 and Z907 carrier generations were minimal in the fabricated devices, while influence of 4T dye on carrier generation was dominant, with the peak external quantum efficiency over 60% higher than the peak absorption of 4T dye. This is probably attributed to the improved hole-mobility caused by the 4T dye and better compatibility of the oligothiophene dye with the poly(3-hexyl thiophene) polymer.

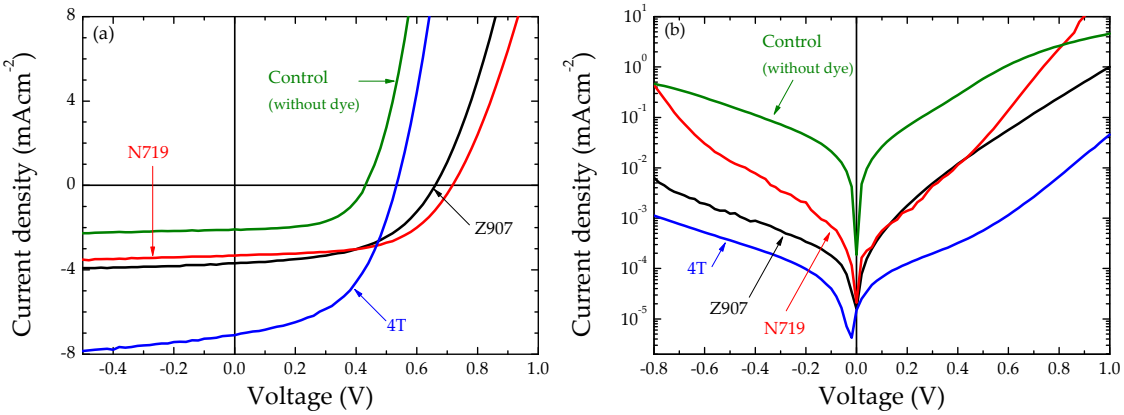

Figure 4. (**a**) J-V characteristics of the fabricated TiO_2/P3HT and dye-modified TiO_2/P3HT solar cells under simulated irradiation of 100 mW cm^{-2} (1 sun) with Air Mass 1.5 filter and (**b**) semi-log J-V plot of the solar cells in dark. The complete structure of control device is ITO/TiO_2/P3HT/Au, and the dye modified cells have the structure ITO/TiO_2/dye/P3HT/Au. Here, dyes Z907, N719, and 4T were used as the interface modifiers.

Table 1. Current density vs. voltage measurement data for the control device and other corresponding dye-modified devices.

Condition	$J_{SC}(mAcm^{-2})$	$V_{OC}(V)$	FF%	Efficiency %
Without dye (control)	2.09	0.44	44	0.41
N719	3.33	0.65	39	0.86
Z907	3.70	0.71	38	1.01
4T	7.30	0.57	49	2.04

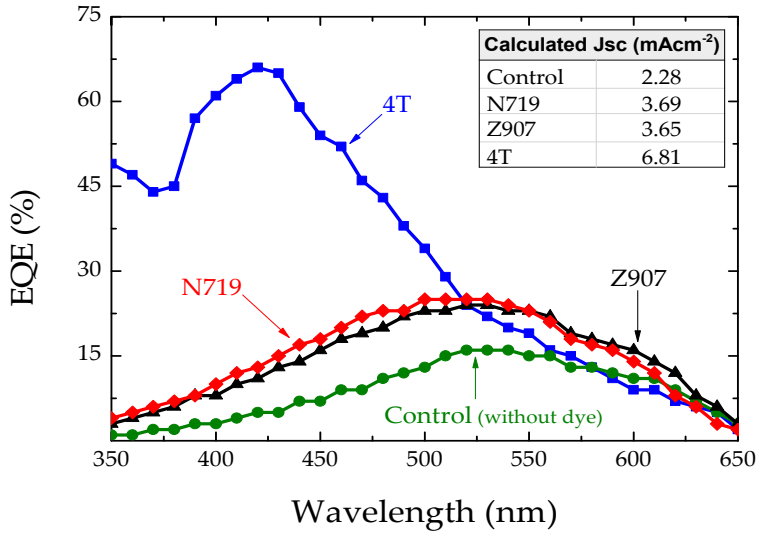

Figure 5. External quantum efficiency (EQE) of ITO/TiO_2/P3HT/Au (control) and ITO/TiO_2/dye/P3HT/Au (interface-modified) solar cells. Here, the dyes Z907, N719, and 4T were used as the interface modifiers in TiO_2/P3HT solar cells. The inset table presents the calculated short circuit current density (J_{SC}) from the EQE graph.

Further, Figure 4 shows that dye treatment, especially 4T dye, significantly suppressed the dark current and increased both the V_{OC} and J_{SC} under simulated solar irradiation, relative to the case of the device without dye. This is consistent with the schematic energy band diagram of the TiO_2/4T/P3HT device shown in the Figure 6, where deep LUMO levels of 4T relative to P3HT were present. The 4T layer was expected to obstruct hole transfer between P3HT and TiO_2, and thus to localize hole-polarons in the P3HT away from the TiO_2 surface. Energy levels for TiO_2 [18], 4T [16], and P3HT [16,18,39] in Figure 6 were directly taken from literature.

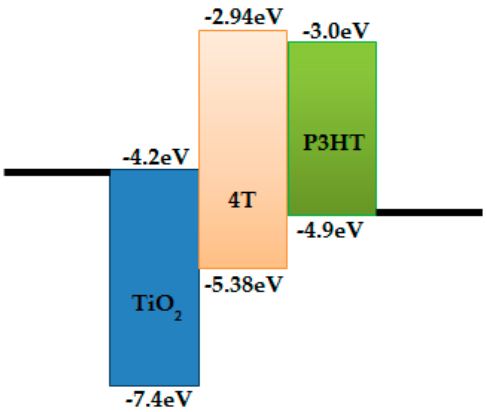

Figure 6. Schematic energy band diagram of the TiO_2/4T/P3HT solar cell.

As in Figure 3a, the extinction coefficient of the 4T dye was higher than that of N719 and Z907 dyes. To find the optimum dye concentration for maximum energy conversions, TiO_2 electrodes with different concentrations of 4T dye were studied. Figure 7 summarizes the variation of photon conversion efficiencies (PCEs) of six cells fabricated with three different concentrations of 4T dye. The average power conversion efficiency was at maximum at 0.15 mM, with a champion efficiency over 2.0%. Table 2 compares the PCEs of solar cells in this work with recently reported TiO_2/P3HT solar cells with various interface modifiers including dyes. The Table 1 clearly shows that the 4T dye-modified devices showed the best PCE of devices with pristine P3HT and nanoporous TiO_2 electrodes. It should be noted that our devices have TiO_2 nanoparticles which did not undergo $TiCl_4$ treatment.

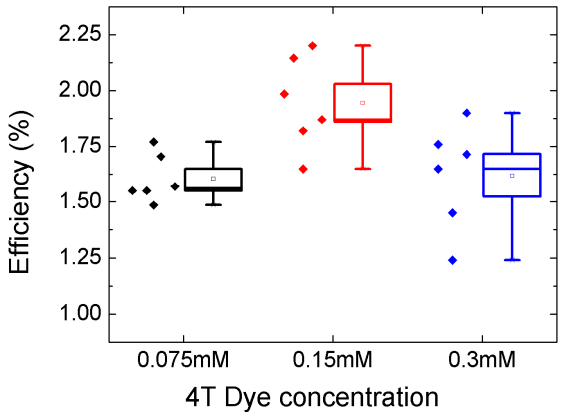

Figure 7. Distribution of power conversion efficiencies of six cells fabricated with three different concentrations (box indicates the standard deviations, whiskers indicate the range, and the small square in the middle of each box indicates the average).

Table 2. Photon conversion efficiencies (PCEs) of recently reported TiO_2/P3HT solar cells with various interface modifiers including dyes.

Device Structure—Different Interface Modifiers	Efficiency %	Year	Reference
TiO_2/carboxylated oligothiophene/P3HT	0.11	2015	[28]
TiO_2/BT5 oligomer/P3HT	0.21	2019	[10]
$TiCl_4$ treatment/TiO_2 nanorod/ACA/P3HT	0.28	2015	[40]
TiO_2/$TiCl_4$ treatment/[6,6]-Phenyl C61 butyric acid/P3HT	0.37	2015	[41]
TiO_2/$TiCl_4$ treatment/D131/P3HT	1.53	2015	[41]
TiO_2/$TiCl_4$ treatment/squaraine dye SQ2/P3HT	2.22	2015	[41]
TiO_2 nanorod/P3HT/PEDOT:PSS	0.43	2012	[15]
TiO_2 nanorod(650 nm)/D149/P3HT/PEDOT:PSS	1.58	2012	[15]
TiO_2 nanorod(1.5 µm)/D149/P3HT/PEDOT:PSS	3.12	2012	[15]
TiO_2 nanorod/Z907/P3HT/PEDOT:PSS	0.94	2012	[15]
TiO_2 nanowires/Pyridine/P3HT	0.45	2015	[42]
TiO_2/Z907/P3HT/PEDOT:PSS	0.53	2017	[35]
TiO_2 nanowires/$TiCl_4$ treatment/CdS/P3HT	0.7	2015	[42]
TiO_2 nanofibers/N719/P3HT	0.90	2010	[43]
TiO_2/Nitro Benzoic Acid treatment/P3HT/PEDOT:PSS	1.05	2017	[3]
TiO_2 nanofibers/N719 + PPA/P3HT	1.09	2010	[43]
TiO_2/Methoxy Benzoic Acid treatment/P3HT/PEDOT:PSS	1.24	2017	[3]
TiO_2/Al_2O_3/N719/P3HT/PEDOT:PSS	1.4	2014	[38]
TiO_2/$TiCl_4$ treatment/4T/doped P3HT	1.54	2014	[16]
TiO_2/$TiCl_4$ treatment/5T/doped P3HT	2.32	2014	[16]
TiO_2 nanorod/$TiCl_4$ treatment/D149/TBP/P3HT/PEDOT:PSS	1.83	2012	[44]
TiO_2/triphenylamine dye/P3HT	2.01	2016	[45]
TiO_2/Z907/P3HT	1.01	2019	Current work
TiO_2/N719/P3HT	0.86	2019	Current work
TiO_2/4T/P3HT	2.04	2019	Current work

4. Conclusions

Three different dyes, including a metal-free 4T dye as an interface modifier on TiO_2/P3HT solar cells, were investigated. It was found that the commercial dyes N719 and Z907 improved the performance of the solar cells by improving the hole-mobility of the polymer and by reducing the back-electron transfer at the interface. Among all the dyes used, the insertion of 4T dye improved the efficiency by five-fold, which was higher when compared to other dyes used. Optimized nanoporous TiO_2/P3HT solar cells with 4T dye yielded maximum efficiency over 2% under 1 sun illumination with an AM 1.5 filter. This is attributed to a combination of charge carrier generation due to 4T dye, as shown by EQE spectra data, and improved morphology and mobility of the P3HT caused by the 4T.

Supplementary Materials: The following are available online at http://www.mdpi.com/2073-4360/11/11/1752/s1, Figure SM1: Cross sectional FESEM image for fabricated TiO_2/4T/P3HT solar cell. The thickness of ITO layer was found to be 201.2 nm, Figure SM2: Cross sectional FESEM image for fabricated TiO_2/4T/P3HT solar cell with individual thickness for each layer, Figure SM3: Cross sectional FESEM image for fabricated TiO_2/4T/P3HT solar cell. The thickness of P3HT layer was found to be 177.7 nm, Figure SM4: Cross sectional FESEM image for fabricated TiO_2/4T/P3HT solar cell.

Author Contributions: Conceptualization, A.P., T.M., N.R., P.R. and D.V.; Data curation, A.P., T.M., N.R., P.R. and D.V.; Formal analysis, A.P., T.M., N.R., P.R. and D.V.; Funding acquisition, P.R. and D.V.; Investigation, A.P., T.M., N.R., P.R. and D.V.; Methodology, A.P. and T.M.; Project administration, P.R. and D.V.; Resources, N.R., P.R. and D.V.; Software, A.P. and T.M.; Supervision, N.R., P.R. and D.V.; Validation, A.P., T.M., N.R., P.R. and D.V.; Visualization, P.R. and D.V.; Writing – original draft, A.P.; Writing – review & editing, T.M., N.R., P.R. and D.V.

Funding: This research was funded by Capacity Building and Establishment of a Research Consortium (CBERC) project, grant number LKA-3182-HRNCET and Higher Education and Research collaboration on Nanomaterials for Clean Energy Technologies (HRNCET) project, grant number NORPART/2016/10237.

Conflicts of Interest: The authors declare no conflict of interest.

References

1. Tountas, M.; Topal, Y.; Verykios, A.; Soultati, A.; Kaltzoglou, A.; Papadopoulos, T.A.; Tsikritzis, D. A silanol-functionalized polyoxometalate with excellent electron transfer mediating behavior to ZnO and TiO2cathode interlayers for highly efficient and extremely stable polymer solar cells. *J. Mater. Chem. C* **2018**, *6*, 1459–1469. [CrossRef]
2. Wright, M.; Uddin, A. Organic—inorganic hybrid solar cells: A comparative review. *Sol. Energy Mater. Sol. Cells* **2012**, *107*, 87–111. [CrossRef]
3. Loheeswaran, S.; Thanihaichelvan, M.; Ravirajan, P.; Nelson, J. Controlling recombination kinetics of hybrid poly-3-hexylthiophene (P3HT)/titanium dioxide solar cells by self-assembled monolayers. *J. Mater. Sci. Mater. Electron.* **2017**, *28*, 4732–4737. [CrossRef]
4. Eom, S.H.; Baek, M.J.; Park, H.; Yan, L.; Liu, S.; You, W.; Lee, S.H. Roles of interfacial modifiers in hybrid solar cells: Inorganic/polymer bilayer vs inorganic/polymer:Fullerene bulk heterojunction. *ACS Appl. Mater. Interfaces* **2014**, *6*, 803–810. [CrossRef]
5. Ravirajan, P.; Haque, S.A.; Durrant, J.R.; Bradley, D.D.C.; Nelson, J. The effect of polymer optoelectronic properties on the performance of multilayer hybrid polymer/TiO_2solar cells. *Adv. Funct. Mater.* **2005**, *15*, 609–618. [CrossRef]
6. Balashangar, K.; Paranthaman, S.; Thanihaichelvan, M.; Amalraj, P.A.; Velauthapillai, D.; Ravirajan, P. Multi-walled carbon nanotube incorporated nanoporous titanium dioxide electrodes for hybrid polymer solar cells. *Mater. Lett.* **2018**, *219*, 265–268. [CrossRef]
7. Ishwara, T.; Bradley, D.D.C.; Nelson, J.; Ravirajan, P.; Vanseveren, I.; Cleij, T.; Vanderzande, D.; Lutsen, L.; Tierney, S.; Heeney, M.; et al. Influence of polymer ionization potential on the open-circuit voltage of hybrid polymer/ Ti O2 solar cells. *Appl. Phys. Lett.* **2008**, *92*, 48–51. [CrossRef]
8. Prashanthan, K.; Thivakarasarma, T.; Ravirajan, P.; Planells, M.; Robertson, N.; Nelson, J. Enhancement of hole mobility in hybrid titanium dioxide/poly(3-hexylthiophene) nanocomposites by employing an oligothiophene dye as an interface modifier. *J. Mater. Chem. C* **2017**, *5*, 11758–11762. [CrossRef]
9. Wu, F.; Zhu, Y.; Ye, X.; Li, X.; Tong, Y.; Xu, J. Balanced Dipole Effects on Interfacial Engineering for Polymer/TiO2 Array Hybrid Solar Cells. *Nanoscale Res. Lett.* **2017**, *12*, 85. [CrossRef] [PubMed]

10. Mecking, S.; Schmidt-Mende, L.; Ehrenreich, P.; Groh, A.; Huster, J.; Goodwin, H.; Deschler, F. Tailored Interface Energetics for Efficient Charge Separation in Metal Oxide-Polymer Solar Cells. *Sci. Rep.* **2019**, *9*, 1–11.
11. Peiró, A.M.; Ravirajan, P.; Govender, K.; Boyle, D.S.; O'Brien, P.; Bradley, D.D.C.; Nelson, J.; Durrant, J.R. The effect of zinc oxide nanostructure on the performance of hybrid polymer/zinc oxide solar cells. *Proc. SPIE - Int. Soc. Opt. Eng.* **2005**, *5938*, 593819.
12. Armstrong, C.L.; Price, M.B.; Munoz-Rojas, D.; Davis, N.J.K.L.; Abdi-Jalebi, M.; Friend, R.H.; Greenham, N.C.; MacManus-Driscoll, J.L.; Boehm, M.L.; Musselman, K.P. Influence of an Inorganic Inter layer on Exciton Separation in Hybrid Solar Cells. *ACS Nano* **2015**, *9*, 11863–11871. [CrossRef] [PubMed]
13. Bouclé, J.; Ravirajan, P.; Nelson, J. Hybrid polymer-metal oxide thin films for photovoltaic applications. *J. Mater. Chem.* **2007**, *17*, 3141–3153. [CrossRef]
14. Ravirajan, P.; Atienzar, P.; Nelson, J. Post-Processing Treatments in Hybrid Polymer/Titanium Dioxide Multilayer Solar Cells. *J. Nanoelectron. Optoelectron.* **2012**, *7*, 498–502. [CrossRef]
15. Liao, W.; Hsu, S.; Lin, W.; Wu, J. Hierarchical TiO_2 Nanostructured Array/P3HT Hybrid Solar Cells with Interfacial Modification. *J. Phys. Chem. C* **2012**, *116*, 15938–15945. [CrossRef]
16. Planells, M.; Abate, A.; Snaith, H.J.; Robertson, N. Oligothiophene interlayer effect on photocurrent generation for hybrid TiO2/P3HT Solar Cells. *ACS Appl. Mater. Interfaces* **2014**, *6*, 17226–17235. [CrossRef] [PubMed]
17. Lo, S.; Liu, Z.; Li, J.; Chan, H.L.; Yan, F. Progress in Natural Science: Materials International Hybrid solar cells based on poly (3-hexylthiophene) and electrospun TiO_2 nano fibers modi fied with CdS nanoparticles. *Progress Nat. Sc.: Mater. Int.* **2013**, *23*, 514–518. [CrossRef]
18. Thanihaichelvan, M.; Sockiah, K.; Balashangar, K.; Ravirajan, P. Cadmium sulfide interface layer for improving the performance of titanium dioxide/poly (3-hexylthiophene) solar cells by extending the spectral response. *J. Mater. Sci. Mater. Electron.* **2015**, *26*, 3558–3563. [CrossRef]
19. Thanihaichelvan, M.; Sri Kodikara, M.M.P.; Ravirajan, P.; Velauthapillai, D. Enhanced performance of nanoporous titanium dioxide solar cells using cadmium sulfide and poly(3-hexylthiophene) co-sensitizers. *Polymers* **2017**, *9*, 467. [CrossRef]
20. Senthil, T.S.; Muthukumarasamy, N.; Velauthapillai, D.; Agilan, S.; Thambidurai, M.; Balasundaraprabhu, R. Natural dye (cyanidin 3-O-glucoside) sensitized nanocrystalline TiO2 solar cell fabricated using liquid electrolyte/quasi-solid-state polymer electrolyte. *Renew. Energy* **2011**, *36*, 2484–2488. [CrossRef]
21. Gokilamani, N.; Muthukumarasamy, N.; Thambidurai, M.; Ranjitha, A.; Velauthapillai, D. Utilization of natural anthocyanin pigments as photosensitizers for dye-sensitized solar cells. *J. Sol.-Gel Sci. Technol.* **2013**, *66*, 212–219. [CrossRef]
22. Prabavathy, N.; Shalini, S.; Balasundaraprabhu, R.; Velauthapillai, D.; Prasanna, S.; Muthukumarasamy, N. Enhancement in the photostability of natural dyes for dye-sensitized solar cell (DSSC) applications: A review. *Int. J. Energy Res.* **2017**, *41*, 1372–1396. [CrossRef]
23. Akila, Y.; Muthukumarasamy, N.; Agilan, S.; Mallick, T.K.; Senthilarasu, S.; Velauthapillai, D. Enhanced performance of natural dye sensitised solar cells fabricated using rutile TIO_2 nanorods. *Opt. Mater. (Amst)* **2016**, *58*, 76–83. [CrossRef]
24. Ramakrishnan, V.M.; Natarajan, M.; Santhanam, A.; Asokan, V.; Velauthapillai, D. Size controlled synthesis of TiO2nanoparticles by modified solvothermal method towards effective photo catalytic and photovoltaic applications. *Mater. Res. Bull.* **2018**, *97*, 351–360. [CrossRef]
25. Wang, P.; Zakeeruddin, S.M.; Humphry-Baker, R.; Moser, J.E.; Grätzel, M. Molecular-Scale Interface Engineering of TiO_2 Nanocrystals: Improving the Efficiency and Stability of Dye-Sensitized Solar Cells. *Adv. Mater.* **2003**, *15*, 2101–2104. [CrossRef]
26. Wang, Z.S.; Kawauchi, H.; Kashima, T.; Arakawa, H. Significant influence of TiO2 photoelectrode morphology on the energy conversion efficiency of N719 dye-sensitized solar cell. *Coord. Chem. Rev.* **2004**, *248*, 1381–1389. [CrossRef]
27. Zhong, M.; Yang, D.; Zhang, J.; Shi, J.; Wang, X.; Li, C. Improving the performance of CdS/P3HT hybrid inverted solar cells by interfacial modification. *Sol. Energy Mater. Sol. Cells* **2012**, *96*, 160–165. [CrossRef]
28. Reeja-Jayan, B.; Koen, K.A.; Ono, R.J.; Vanden Bout, D.A.; Bielawski, C.W.; Manthiram, A. Oligomeric interface modifiers in hybrid polymer solar cell prototypes investigated by fluorescence voltage spectroscopy. *Phys. Chem. Chem. Phys.* **2015**, *17*, 10640–10647. [CrossRef]

29. Kan, B.; Li, M.; Zhang, Q.; Liu, F.; Wan, X.; Wang, Y.; Ni, W.; Long, G.; Yang, X.; Feng, H.; et al. A series of simple oligomer-like small molecules based on oligothiophenes for solution-processed solar cells with high efficiency. *J. Am. Chem. Soc.* **2015**, *137*, 3886–3893. [CrossRef]
30. Hu, Y.; Ivaturi, A.; Planells, M.; Boldrini, C.L.; Biroli, A.O.; Robertson, N. "Donor-free" oligo(3-hexylthiophene) dyes for efficient dye-sensitized solar cells. *J. Mater. Chem. A* **2016**, *4*, 2509–2516. [CrossRef]
31. Wang, P.; Klein, C.; Humphry-Baker, R.; Zakeeruddin, S.M.; Graetzel, M. A high molar extinction coefficient sensitizer for stable dye-sensitized solar cells. *J. Am. Chem. Soc.* **2005**, *127*, 808–809. [CrossRef] [PubMed]
32. Abate, A.; Planells, M.; Hollman, D.J.; Stranks, S.D.; Petrozza, A.; Kandada, A.R.S.; Vaynzof, Y.; Pathak, S.K.; Robertson, N.; Snaith, H.J. An organic "donor-free" dye with enhanced open-circuit voltage in solid-state sensitized solar cells. *Adv. Energy Mater.* **2014**, *4*, 1400166. [CrossRef]
33. Pitchaiya, S.; Natarajan, M.; Santhanam, A.; Asokan, V.; Madurai Ramakrishnan, V.; Selvaraj, Y.; Yuvapragasam, A.; Rangasamy, B.; Sundaram, S.; Velauthapillai, D. The Performance of $CH_3NH_3PbI_3$ - Nanoparticles based – Perovskite Solar Cells Fabricated by Facile Powder press Technique. *Mater. Res. Bull.* **2018**, *108*, 61–72. [CrossRef]
34. Uthayaraj, S.; Karunarathne, D.; Kumara, G.; Murugathas, T.; Rasalingam, S.; Rajapakse, R.; Ravirajan, P.; Velauthapillai, D. Powder Pressed Cuprous Iodide (CuI) as A Hole Transporting Material for Perovskite Solar Cells. *Materials* **2019**, *12*, 2037. [CrossRef] [PubMed]
35. Ishwara, T. Comparison of TiO_2 Nanoporous Films in Hybrid Organic-inorganic Solar Cells. *Energy Procedia* **2017**, *110*, 109–114. [CrossRef]
36. Xu, B.; Sai-Anand, G.; Gopalan, A.I.; Qiao, Q.; Kang, S.W. Improving photovoltaic properties of P3HT:IC60BA through the incorporation of small molecules. *Polymers* **2018**, *10*, 121. [CrossRef]
37. Mahmood, A.; Khan, S.U.D.; Rana, U.A.; Janjua, M.R.S.A.; Tahir, M.H.; Nazar, M.F.; Song, Y. Effect of thiophene rings on UV/visible spectra and non-linear optical (NLO) properties of triphenylamine based dyes: A quantum chemical perspective. *J. Phys. Org. Chem.* **2015**, *28*, 418–422. [CrossRef]
38. Loheeswaran, S.; Balashangar, K.; Jevirshan, J.; Ravirajan, P. Controlling Recombination Kinetics of Hybrid Nanocrystalline Titanium Dioxide/Polymer Solar Cells by Inserting an Alumina Layer at the Interface. *J. Nanoelectron. Optoelectron.* **2014**, *8*, 484–488. [CrossRef]
39. Ravirajan, P.; Peir, A.M.; Nazeeruddin, M.K.; Graetzel, M.; Bradley, D.D.C.; Durrant, J.R.; Nelson, J.; Peiro, A.M. Hybrid Polymer/Zinc Oxide Photovoltaic Devices with Vertically Oriented ZnO Nanorods and an Amphiphilic Molecular Interface Layer Hybrid Polymer/Zinc Oxide Photovoltaic Devices with Vertically Oriented ZnO Nanorods and an Amphiphilic Molecular Interfa. *J. Phys. Chem.* **2006**, *110*, 7635–7639. [CrossRef]
40. Wang, D.; Tao, H.; Zhao, X.; Ji, M.; Zhang, T. Enhanced photovoltaic performance in TiO2/P3HT hybrid solar cell by interface modification. *J. Semicond.* **2015**, *36*, 023006. [CrossRef]
41. Ehrenreich, P.; Pfadler, T.; Paquin, F.; Dion-Bertrand, L.I.; Paré-Labrosse, O.; Silva, C.; Weickert, J.; Schmidt-Mende, L. Role of charge separation mechanism and local disorder at hybrid solar cell interfaces. *Phys. Rev. B - Condens. Matter Mater. Phys.* **2015**, *91*, 035304. [CrossRef]
42. Wang, D.; Han, J.; Zhang, T.; Zhao, X.; Tao, H. TiO_2/P3HT Hybrid Solar Cell with Efficient Interface Modification by Organic and Inorganic Materials: A Comparative Study. *J. Nanosci. Nanotechnol.* **2015**, *16*, 797–801. [CrossRef] [PubMed]
43. Tai, Q.; Zhao, X.; Yan, F. Hybrid solar cells based on poly(3-hexylthiophene) and electrospun TiO_2 nanofibers with effective interface modification. *J. Mater. Chem.* **2010**, *20*, 7366–7371. [CrossRef]
44. Hsu, S.; Liao, W.; Lin, W.; Wu, J. Modulation of Photocarrier Dynamics in Indoline Dye-Modified TiO 2 Nanorod Array/P3HT Hybrid Solar Cell with 4- tert -Butylpridine. *J. Phys. Chem. C* **2012**, *116*, 25721–25726. [CrossRef]
45. Pei, J.; Hao, Y.Z.; Lv, H.J.; Sun, B.; Li, Y.P.; Guo, Z.M. Optimizing the performance of TiO_2/P3HT hybrid solar cell by effective interfacial modification. *Chem. Phys. Lett.* **2016**, *644*, 127–131. [CrossRef]